Electronically Driven Structure Changes of Si Captured by Femtosecond Electron Diffraction

Maher Harb,[1] Ralph Ernstorfer,[1] Christoph T. Hebeisen,[1] Germán Sciaini,[1] Weina Peng,[2] Thibault Dartigalongue,[1] Mark A. Eriksson,[2] Max G. Lagally,[2] Sergei G. Kruglik,[1] and R. J. Dwayne Miller[1,*]

[1]*Institute for Optical Sciences and Departments of Physics and Chemistry, University of Toronto, 80 St. George Street, Toronto, Ontario M5S 3H6, Canada*

[2]*University of Wisconsin–Madison, Madison, Wisconsin 53706, USA*

(Received 19 December 2007; published 18 April 2008)

The excitation of a high density of carriers in semiconductors can induce an order-to-disorder phase transition due to changes in the potential-energy landscape of the lattice. We report the first direct resolution of the structural details of this phenomenon in freestanding films of polycrystalline and (001)-oriented crystalline Si, using 200-fs electron pulses. At excitation levels greater than ~6% of the valence electron density, the crystalline structure of the lattice is lost in <500 fs, a time scale indicative of an electronically driven phase transition. We find that the relaxation process along the modified potential is not inertial but rather involves multiple scattering towards the disordered state.

DOI: 10.1103/PhysRevLett.100.155504 PACS numbers: 61.05.J−, 64.60.−i

For the most part, strongly driven phase transitions involve simple lattice heating through the picosecond dynamics of converting absorbed light energy into atomic motions. With short enough laser pulses, however, it is possible to change the electron distribution within an effectively cold underlying lattice and probe how these changes affect the bonding forces that hold the lattice together. Typically, bond softening occurs due to the increased antibonding character of the excited charge distribution. At some excitation level, the interatomic potential-energy surface becomes repulsive and the lattice undergoes bond displacements and eventual bond breaking to form a disordered state. This process has been referred to as nonthermal melting as it occurs before thermal equilibrium is attained between electrons and lattice through electron-phonon interactions. There are, however, fundamental differences in bonding for different types of materials, as well as differences in electron relaxation dynamics that compete against an electronically induced phase transition. For example, Al, a metal with a face-centered cubic lattice structure, is stabilized by a uniform electron distribution within the periodic positive potential of the nuclei. There is no directional bonding between Al atoms, and the process of electron relaxation is extremely fast. The structural changes of Al are best described as a thermally propagated phase transition [1,2]. In contrast, Si is a semiconductor with a diamond structure that involves highly directional bonding between atoms through the sp^3 hybridized band states. The energy band gap greatly retards electron relaxation and enhances the separation of electronic and thermal factors influencing the lattice dynamics. Given the importance of Si in driving the solid state electronics revolution, the prospect of modifying the lattice potential and the associated band structure on ultrashort time scales is an intriguing proposition, both for its fundamental new insights into the atomic forces at play and for possible applications.

Experimentally, the challenge is to determine the effects of the electronically induced changes in bonding on the lattice. The very first experiments used all-optical methods to observe the onset of liquidlike optical properties within a few hundred femtoseconds as a measure of the structural phase transition [3–5]. Changes in optical properties are related to changes in the electronic distribution, and it has remained an open question whether these changes were a direct consequence of structural changes. In contrast, time resolved electron [1,6,7] and x-ray [8–12] diffraction are ideal tools, as they provide a direct mapping of the lattice structure. There has been a number of seminal contributions to the study of electronically driven structural changes in semiconductors starting with the work of Siders *et al.* on the nonthermal melting of Ge using hard-1.54 Å x rays with ps time resolution [8]. Recent efforts focused on InSb taking advantage of the higher diffraction cross section associated with high Z materials [9,11,12]. Yet, Si remains an important test case as the band structure and the associated potential-energy surfaces for the lattice stability of Si are better understood than virtually any other material.

The primary challenge in femtosecond electron diffraction is minimizing the temporal broadening of the electron pulses due to space charge. While it is possible to circumvent this problem by using a low number of electrons per pulse, structural phase transitions under strongly driven conditions lead to nonreversible changes in the sample and one quickly runs out of usable sample long before enough diffraction signal is acquired. Our approach has been to minimize the effects of space charge through a compact gun design, with 3 cm of propagation between photocathode and sample. The current setup, shown in

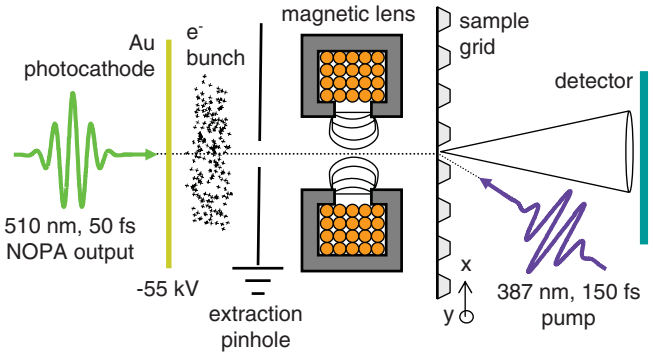

FIG. 1 (color). Schematic of the experimental setup. Electrons are generated via 2-photon photoemission from a Au photocathode and accelerated to 55 keV. A magnetic lens collimates the electron beam prior to scattering off the freestanding Si films at a distance of approximately 3 cm from the photocathode. The diffraction pattern is detected on a microchannel plate/phosphor screen and recorded with a charge-coupled device camera.

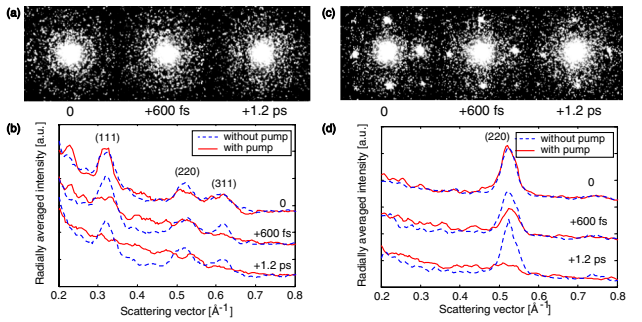

FIG. 2 (color online). Raw diffraction images of the polycrystalline (a) and the (001)-oriented crystalline (c) Si membranes shown for selected time delays relative to the pump pulse, and the corresponding radially averaged intensity profiles (solid lines) and reference profiles taken without excitation (dashed lines), for polycrystalline (b) and (001)-oriented crystalline (d) Si. As nonreversible sample damage is incurred by a single laser shot, the diffraction images presented were averaged over 8–11 shots, each taken at a fresh sample position.

Fig. 1, delivers, at the sample position, 200-fs pulses containing ~6000 electrons focused to a 150 μm spot. The electron pulse duration was characterized using the recently developed electron-laser pulse cross-correlation method based on ponderomotive scattering [13]. Photoinduced changes in Si were initiated by 387-nm, 150-fs pump pulses focused to 230 μm. Taking the duration of the optical pump pulse into account, the overall instrumental response time is better than 300 fs (FWHM).

Another important feature of the present experiment was the use of nanofabrication methods to develop 50 nm and 30 nm freestanding films of polycrystalline and (001)-oriented crystalline Si, respectively. The fabrication process of the polycrystalline samples is described in detail elsewhere [14]. The fabrication and transfer of the freestanding films of crystalline Si is described in Refs. [15,16]. The outer Si layer of silicon on insulator is repeatedly thinned by controlled oxidation and etching in HF to remove the oxide. The thickness of this Si layer is verified by x-ray diffraction. The Si film is patterned and subsequently removed from the Si handle wafer by etching the buried-oxide layer and transferred onto cleaned Si grids for use in diffraction measurements in transmission geometry.

Figure 2(a) presents raw diffraction patterns of polycrystalline Si taken at selected time points relative to the arrival of the excitation pulse, at an absorbed fluence of 65 mJ/cm^2. Assuming a single-photon absorption process across the direct band gap of Si of 3.4 eV [17], at this excitation level ~11% of the valence electrons are promoted to the conduction band. The corresponding radially averaged intensity profiles shown in Fig. 2(b) exhibit two clear features: a loss in the intensity of Bragg peaks and an increase in intensity between the (111) and the (220) peaks. In a polycrystalline structure, these features are due to either heating or an order-to-disorder phase transition [18]. Lattice heating reduces the diffracted intensity according to the Debye-Waller (DW) model,

$$I = I_0 \exp\left[-\frac{(2\pi s)^2\langle u^2\rangle}{3}\right], \qquad (1)$$

where I is the diffracted intensity, s is the magnitude of the scattering vector, and $\langle u^2\rangle$ is the atomic mean-square displacement [19]. At the melting temperature of Si of 1687 K, we estimate, using $\langle u^2\rangle$ based on parametrization by Gao [20], that the DW effect accounts for a loss of 14%, 33%, and 42% in the amplitudes of the (111), (220), and (311) peaks, respectively. In contrast, the measured intensity profiles display, early on, a complete loss of order characteristic of a phase transition, and the emergence of a broad structure in a scattering range where no diffraction orders exist. At longer time delays (up to the delay stage limit of ~1 ns) no significant change in the diffraction pattern was observed, indicating that the initially created disordered state of Si rapidly attains the fully relaxed structure to the new charge distribution. X-ray based structure factor measurements of pure liquid Si reveal a broad peak in the 0.3–0.6 Å^{-1} range [21], exactly as observed in this study for excitation conditions above the melting threshold. The onset of the phase transition is more pronounced in the diffraction pattern of the (001)-oriented crystalline Si samples than the polycrystalline samples due to the much higher diffraction intensity in the (220) spots relative to background as shown in Fig. 2(c). The observed dynamics appear as intensity shifts from the (220) spots to uniformly distributed regions in a broad s range. Typically, heating effects in single crystalline structures take on the form of streaks [18]. In contrast, the observed transformation from a fourfold to a radial symmetry indicates a loss of orientation consistent with a phase transition to a liquidlike disordered state.

The different diffraction orders are found to decay concertedly for polycrystalline Si as shown in Fig. 3(a) and

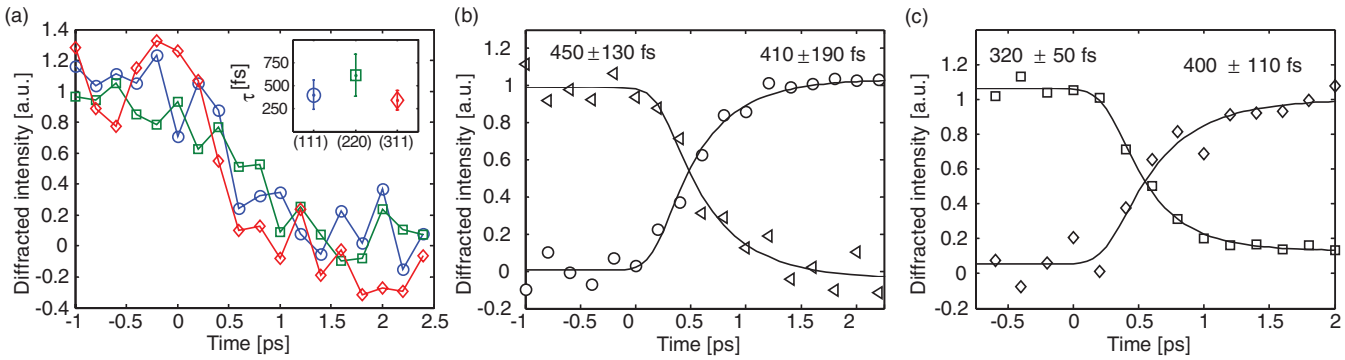

FIG. 3 (color). Kinetics of electron diffraction at ~11% valence excitation. The normalized decays of the different diffraction orders of polycrystalline Si: (111) peak, circles; (220) peak, squares; (311) peak, diamonds (a). The inset of (a) shows the corresponding decay time constants. The decay of the combined diffracted intensity of the (111), (220), and (311) Bragg peaks (triangles) and the rise of the scattering intensity in the 0.39–0.47 Å^{-1} range (circles) for polycrystalline Si (b). The decay of the (220) Bragg peak (squares) and the rise of the scattering intensity in the 0.22–0.60 Å^{-1} range (diamonds) for (001)-oriented crystalline Si (c). The solid lines are fits to the data points using an exponential decay (rise) function convolved with the 300 fs instrumental response function (reflecting contributions from the 200 fs electron probe and the 150 fs excitation pulse). The displayed time constants in the inset of (a) and in (b) and (c) are those of the exponential component of the fitting function.

thus report on the fraction of the lattice remaining in the diamond structure. To improve S/N, the time dependence of the diffraction signal was calculated by averaging the peak amplitudes of the first three diffraction orders and normalizing by the total detected electron count. These results are shown in Fig. 3(b) for the polycrystalline Si data in which the decay in the diffraction orders associated with the diamond lattice structure and the rise in the scattering intensity between the (111) and (220) peaks associated with disorder are 1:1 correlated. The data were fitted with the convolution function $G \otimes E$, where G is a Gaussian function with a fixed FWHM set to the instrumental response time of 300 fs, and E is a mono-exponential decay function defined as $E = \pm A(1 - \exp[-(t - t_0)/\tau])H(t - t_0) + B$, with B the baseline at negative time points, A the steady-state loss (gain) in amplitude, τ the time constant, and $H(t - t_0)$ the Heaviside step function. The diffraction signal from the initial lattice configuration was found to decay in 450 ± 130 fs, accompanied by a rise in scattering intensity between the (111) and (220) peaks with a time constant of 410 ± 190 fs. The decay of the (220) diffraction order and the rise in scattering intensity in the 0.22–0.60 Å^{-1} range [image sectors corresponding to (220) spots excluded from the radially averaged intensity profiles] are shown in Fig. 3(c) for the (001)-oriented crystalline samples. Here, the localization of the diffracted intensity into well defined directions translates into better S/N. As a consequence, the extracted decay time constant of 320 ± 50 fs has smaller experimental error. The agreement in the rates of disordering between oriented and polycrystalline samples indicates that local effects at the grain boundaries do not contribute significantly to the dynamics. In both types of samples, the sub-500 fs dynamics cannot be explained by the thermal relaxation mechanisms that transfer heat from the hot carriers to the lattice on a time scale of a few ps [14,22], indicating that the observed phase transition is electronic in nature.

Lindenberg *et al.* proposed for InSb that the interatomic potential is softened under these high excitation conditions, and atoms move inertially (at a constant velocity) leading to the collapse of the lattice [11]. In this picture, the mean-square displacement in Eq. (1) is proportional to t^2, causing the decay traces of the diffraction peaks to assume a Gaussian profile. We tested this proposition by fitting the kinetics of Fig. 3 to a half-Gaussian function. However, because of the comparable time scales between the photoinduced dynamics and the instrumental response, both types of fits (exponential and half-Gaussian) were satisfactory. At the same time, we estimated, using the DW model, that the decay of the (220) peak in Fig. 3(c) corresponds to an atomic root mean square (rms) displacement $\langle u^2 \rangle^{1/2}$ of ~0.54 Å in 320 fs, resulting in the velocity of 1.7 Å/ps. This is much slower than the 5 Å/ps rms velocity of Si atoms at room temperature, calculated from $[3k_BT/M]^{1/2}$ following the approach of Ref. [11], where M is the mass of the Si atom. Thus, the alternative picture is that of a perturbed (as opposed to a completely flattened) potential-energy surface involving multiple collisions and diffusive sampling of the phase space along the relaxation coordinate to the disordered phase. This picture is consistent with the concerted decay in the different diffraction orders [Fig. 3(a)] that report on a spatially stochastic sampling process leading to disorder. The phonon frequency in Si is higher than in InSb and there may be a small inertial contribution that was not resolved, but it is not a dominant component.

The dependence of kinetics of the polycrystalline Si structure disappearance on the degree of perturbation in the charge distribution is shown in Fig. 4. Theoretical

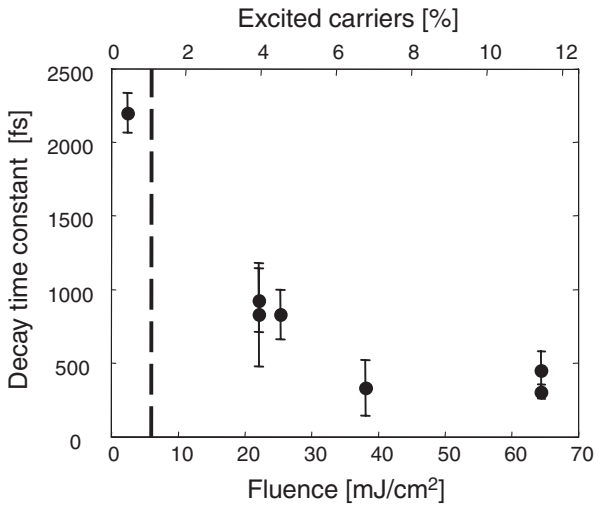

FIG. 4. Dependence of the decay time constant of the combined first three diffraction peaks of polycrystalline Si on the absorbed pump fluence (bottom x axis) and the corresponding electronic excitation level (top x axis). The dashed line at 6 mJ/cm^2 is the observed damage threshold.

studies predict a sharp threshold, in the 5%–10% excitation range, separating the thermal and nonthermal regimes of melting [23–25]. Such an abrupt threshold was not observed in this study. Instead, the intermediate relaxation time constants, observed at 20–30 mJ/cm^2, indicate some electronic contribution to the dynamics. We partially attribute these intermediate time scales to the inhomogeneity of excitation along the film surface due to spatial overlap of pump and probe of comparable sizes. It is also likely that some degree of carrier thermalization and lattice heating is assisting electronically driven disordering in the intermediate excitation range. At excitations below the damage threshold of 6 mJ/cm^2, the heating dynamics are well described by the DW model, with the extracted temperature from the steady-state loss in the peak amplitudes consistent with estimations based on bulk properties of Si. At those excitation levels, the time constant of ~2 ps reflects the purely thermal character of the process with carrier relaxation dominated by carrier screening effects [26], as shown previously [14].

In conclusion, the strongly driven order-to-disorder phase transition of Si is clearly electronically induced, as revealed by our data and as originally proposed [3,23–25], signifying the importance of the highly directional bonding in Si with respect to lattice stability. The resolution of the disordering process demonstrates the power of femtosecond electron diffraction as an atomic probe of structural dynamics. While this methodology is still in its infancy, the present work represents an important milestone with the demonstration of 200 fs electron pulses with sufficient effective brightness for near single shot structure determinations and now avails real time studies of atomic motions involved in the primary events central to chemistry and biology [27].

We thank P. Evans for suggesting the collaboration between the groups, A.-A. Dhirani for use of his deposition chamber, and G. Celler (Soitec, USA) for advice and for supplying SOI materials. We thank Cornell NanoScale Science & Technology Facility and the Emerging Communications Technology Institute at the University of Toronto for use of their nanofabrication facilities. This work was supported by the Natural Sciences and Engineering Research Council of Canada. R. E. thanks the Alexander von Humboldt Foundation for financial support. Support for the University of Wisconsin effort was provided by the U.S. National Science Foundation/MRSEC, Grant No. DMR0520527, and the U.S. Department of Energy, Grant No. DE-FG02-03ER46028.

*dmiller@lphys.chem.utoronto.ca

[1] B. J. Siwick *et al.*, Science **302**, 1382 (2003).
[2] M. Kandyla, T. Shih, and E. Mazur, Phys. Rev. B **75**, 214107 (2007).
[3] V. Shank, R. Yen, and C. Hirlimann, Phys. Rev. Lett. **50**, 454 (1983).
[4] H. W. K. Tom, G. D. Aumiller, and C. H. Brito-Cruz, Phys. Rev. Lett. **60**, 1438 (1988).
[5] K. Sokolowski-Tinten, J. Bialkowski, and D. von der Linde, Phys. Rev. B **51**, 14186 (1995).
[6] J. Cao *et al.*, Appl. Phys. Lett. **83**, 1044 (2003).
[7] C.-Y. Ruan *et al.*, Science **304**, 80 (2004).
[8] C. W. Siders *et al.*, Science **286**, 1340 (1999).
[9] A. Rousse *et al.*, Nature (London) **410**, 65 (2001).
[10] A. Cavalleri *et al.*, Phys. Rev. B **63**, 193306 (2001).
[11] A. M. Lindenberg *et al.*, Science **308**, 392 (2005).
[12] B. Hillyard *et al.*, Phys. Rev. Lett. **98**, 125501 (2007).
[13] C. T. Hebeisen, Opt. Express **16**, 3334 (2008).
[14] M. Harb, J. Phys. Chem. B **110**, 25308 (2006).
[15] M. Roberts *et al.*, Nat. Mater. **5**, 388 (2006).
[16] S. A. Scott and M. G. Lagally, J. Phys. D **40**, R75 (2007).
[17] J. B. Renucci, R. N. Tyte, and M. Cardona, Phys. Rev. B **11**, 3885 (1975).
[18] Z. L. Wang, Micron **34**, 141 (2003).
[19] C. Kittel, *Introduction to Solid State Physics* (Wiley, New York, 1986).
[20] H. X. Gao and L.-M. Peng, Acta Crystallogr. Sect. A **55**, 926 (1999).
[21] Y. Kita *et al.*, J. Phys. Condens. Matter **6**, 811 (1994).
[22] E. J. Yoffa, Phys. Rev. B **21**, 2415 (1980).
[23] R. Biswas and V. Ambegaokar, Phys. Rev. B **26**, 1980 (1982).
[24] P. Stampfli and K. H. Bennemann, Appl. Phys. A **60**, 191 (1995).
[25] T. Dumitrica *et al.*, Phys. Status Solidi B **241**, 2331 (2004).
[26] E. J. Yoffa, Phys. Rev. B **23**, 1909 (1981).
[27] J. R. Dwyer *et al.*, Phil. Trans. R. Soc. A **364**, 741 (2006).